Tracer Transport in Deep Convective Updrafts: Plume Ensemble versus Bulk Formulations

MARK G. LAWRENCE

Department of Atmospheric Chemistry, Max Planck Institute for Chemistry, Mainz, Germany

PHILIP J. RASCH

Climate and Global Dynamics Division, National Center for Atmospheric Research, Boulder, Colorado

(Manuscript received 13 April 2004, in final form 20 December 2004)

ABSTRACT

Two widely used approaches for parameterizing tracer transport based on convective mass fluxes are the plume ensemble formulation (PEF) and the bulk formulation (BF). Here the behavior of these two is contrasted for the specific case in which the BF airmass fluxes are derived as a direct simplification of an explicit PEF. Relative to the PEF, the BF has a greater rate of entrainment of midtropospheric air into the parcels that reach the highest altitudes, and thus is expected to compute less efficient transport of surface-layer tracers to the upper troposphere. In this study, this difference is quantified using a new algorithm for computing mass conserving, monotonic tracer transport for both the BF and PEF, along with a technique for decomposing a bulk mass flux profile into a set of consistent, discrete plumes for use in the PEF. Runs with a 3D global chemistry transport model (MATCH) show that the BF is likely to be an adequate approximation for most tracers with lifetimes of a week or longer. However, for short-lived tracers (lifetimes of a couple days or less) the BF results in significantly less efficient transport to the upper troposphere than the PEF, with differences exceeding 30% on a monthly zonal mean basis. Implications of these results for tropospheric chemistry are discussed.

1. Introduction

It has long been recognized that transport by deep convection can have a substantial impact on O_3 and other chemical tracers in the atmosphere (e.g., Chatfield and Crutzen 1984; Dickerson et al. 1987; Pickering et al. 1990, 1992; Lelieveld and Crutzen 1994; Lawrence et al. 2003a). This is particularly true for short-lived tracers due to the rapid transport in convective updrafts from the surface to the upper troposphere (UT) on time scales of the order of an hour. In global models, the vertical transport of tracers is typically computed based on convective mass fluxes from a deep cumulus convection parameterization. Many different cumulus parameterizations have been developed (e.g., Manabe et al. 1965; Kuo 1965; Arakawa and Schubert 1974; Tiedtke 1989; Kain and Fritsch 1990; Gregory and Rowntree 1990; Moorthi and Suarez 1992; Hack 1994; Pan and Wu 1995; Zhang and McFarlane 1995; Emanuel and Zivkovic-Rothman 1999; Donner et al. 2001). These have primarily focused on the thermodynamic aspects of the column (water vapor and potential temperature), and intercomparisons of various schemes show considerable differences in their thermodynamic characteristics (e.g., Xie et al. 2002).

One of the most widely used approaches to treating convection in global models is the plume ensemble formulation (PEF), conceptually developed in Arakawa and Schubert (1974, hereafter AS74), and implemented in discretized form in large-scale models by Lord et al. (1982), Hack et al. (1984), Grell (1993), and others. In the PEF the convective cloud population in a region is represented by an ensemble of individual representative cumulus clouds (or plumes) of different heights as depicted schematically in Fig. 1a. The original PEF in AS74 was continuous in altitude; the individual discrete plumes used in large-scale model implementations have been referred to by Lord et al. (1982) as subensembles, since each discrete plume corresponds to the set of in-

Corresponding author address: Dr. Mark Lawrence, Dept. of Atmospheric Chemistry, Max Planck Institute for Chemistry, Posfach 3060, D-55020, Mainz, Germany.
E-mail: lawrence@mpch-mainz.mpg.de

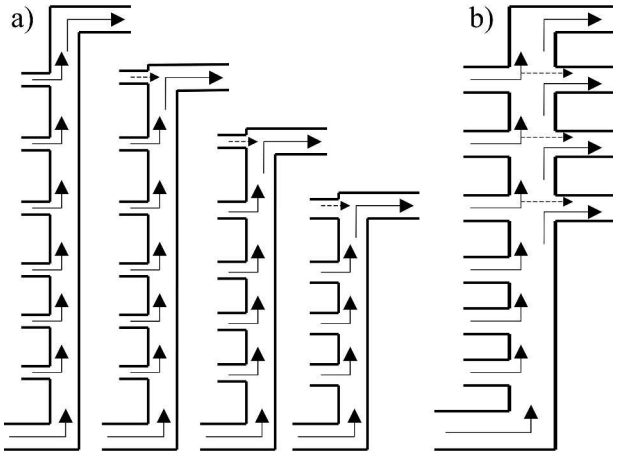

FIG. 1. Schematics of the (a) PEF and (b) BF. Entrainment is represented by arrows entering from the left, detrainment by arrows exiting to the right. There is only a single detrainment layer at the top of the plume for each of the discrete plumes in the PEF. Summing these plumes results in a BF with four detrainment layers in this example.

finitesimal plumes that would detrain in a particular model layer. Each plume has the same base level, and is distinguished only by its rate of entrainment of environmental air,

$$\lambda = \frac{1}{M}\frac{dM}{dz}, \tag{1}$$

where M is the vertical mass flux per unit area and z is the vertical coordinate. Often it is assumed for simplicity that λ is constant for each ensemble member as a function of altitude. Since entrainment reduces a conditionally unstable parcel's buoyancy above the level of free convection, the tallest plume is the one with $\lambda = 0$, and the shortest plume has the maximum allowable λ (which is chosen differently for different realizations of the parameterization). The PEF was the conceptual basis for some of the earliest model studies of the local effects of convection on trace gases (e.g., Chatfield and Crutzen 1984).

An alternative approach to the cumulus parameterization problem is to use the simpler bulk formulation (BF), which explicitly considers only a single entraining and detraining plume (often referred to as a leaky pipe; Fig. 1b). The BF was originally developed for an observational diagnosis study by Yanai et al. (1973; in parallel to the work on the PEF by AS74), and has been implemented in major large-scale models by Bougeault (1985), Tiedtke (1989), Gregory and Rowntree (1990), Grell (1993), Pan and Wu (1995), Zhang and McFarlane (1995), and others. While there are many different possibilities for determining the air and tracer mass fluxes for the BF (cf. Yano et al. 2004), a commonly used approach is to start with a PEF and then sum the entraining plumes together to determine the airmass flux profiles for the BF. These bulk airmass flux profiles are then used in turn to compute the vertical fluxes of water vapor, moist static energy, and tracers.

In this study we will focus only on this special case of a BF that is a direct approximation to a corresponding PEF. Previous tests in the implementations cited above have concluded that this approximation should be adequate for the purpose of simulating water vapor and moist static energy, as well as precipitation and horizontal momentum.

However, this form of the BF has not previously been explicitly tested in comparison with its corresponding PEF for chemical tracers (e.g., O_3, CO, radon, CH_3I, and aerosols), despite the fact that the BF is employed in a wide variety of chemistry transport and chemistry general circulation models, such as MATCH (Rasch et al. 1997; Zhang and McFarlane 1995), CCM3 (Kiehl et al. 1996; Zhang and McFarlane 1995), ECHAM (Roeckner et al. 1999; Tiedtke 1989), TM2, TM3, and TM5 (Heimann 1995; Tiedtke 1989), TOMCAT (Stockwell and Chipperfield 1999; Tiedtke 1989), GEOS/CHEM (Bey et al. 2001; Allen et al. 1996), and STOCHEM (Collins et al. 2002), among others. While for water, the total mixing ratio (vapor plus condensate) at the detrainment level is generally much less than the mixing ratio at the base of the updraft due to condensation and removal of precipitation, no such limitation applies to insoluble tracers. In contrast, an insoluble tracer that is transported from the boundary layer (BL) to the UT in an undiluted (nonentraining) parcel will have the same mixing ratio as it had in the BL (provided chemical losses are not significant on the transport time scale), while a parcel that entrains from the environment can have a very different tracer mixing ratio when it reaches the UT, depending on the environmental vertical profile of the tracer. Air masses in the tallest plumes in the PEF undergo relatively little entrainment, while air masses reaching the highest levels in the BF will have been considerably more diluted by environmental air, because all the plumes are treated together with one mean entrainment rate in the lower parts of the cloud, which is greater than the individual entrainment rates for the tallest plumes of the PEF. Similarly, air masses that detrain at the lowest altitudes in the BF will be less diluted with environmental air than in the PEF. Thus for tracers with surface sources and short lifetimes, so that their mixing ratios decrease significantly with altitude, the BF will transport less of the tracer to the uppermost detrainment levels than the PEF (and more to the lowermost detrainment levels). While the basic

principle of this difference is straightforward, its impact on tracer transport modeling has not yet been quantified in the literature. Thus, we examine the questions: When is the BF an adequate approximation of the PEF for tracer transport, and under which circumstances are the differences in the PEF and a corresponding BF significant enough to favor the use of the more complex PEF in chemistry transport models?

It is important to note that, despite the relative complexity of the PEF compared to the BF, both are nevertheless only crude representations of the actual details of deep cumulus convection within a model column. Evaluating the quality of these and other cumulus parameterizations in comparison to both observations and cloud resolving models is an extensive, ongoing effort of the community, for thermodynamics (e.g., Bechtold et al. 2000; Xie et al. 2002; Yano et al. 2004, etc.) as well as for tracers (e.g., Mahowald et al. 1995; Mari et al. 2000; Bell et al. 2002; Collins et al. 2002; Rasch et al. 2003, etc.) and for other quantities.

We compare the BF and PEF by using representative fictitious tracers with surface sources and five different chemical lifetimes in the global 3D Model of Atmospheric Transport and Chemistry (MATCH), which employs the BF deep convection scheme of Zhang and McFarlane (1995). The next section gives a brief general description of MATCH, and an overview of the technique we have developed for decomposing the bulk mass flux profiles from Zhang and McFarlane (1995) into consistent, discrete plume ensembles, which can then be used for PEF tracer transport in each model column. The section also describes a new scheme for computing bulk and plume ensemble tracer transport that preserves mass and monotonicity, and which includes an optional modification to the BF that helps reduce the differences between it and the PEF. Following that, results are considered from sensitivity runs with MATCH, using the PEF and two realizations of the BF for tracer transport, and the implications for tropospheric chemistry and for future developments in cumulus convection parameterizations are discussed.

2. Model description, convective transport algorithms, and runs setup

a. MATCH

The Model of Atmospheric Transport and Chemistry has been described and evaluated in detail in Rasch et al. (1997), Mahowald et al. (1997a,b), Lawrence et al. (1999b, 2003b), and von Kuhlmann et al. (2003a,b). The model transport and physics parameterizations are mostly based on the CCM3 (Kiehl et al. 1996). MATCH has been used for a variety of studies, including a recent examination of the effects of deep convective transport on global tropospheric O_3 (Lawrence et al. 2003a). Here the basic model setup from Lawrence et al. (2003b) is used, driving the modeled meteorology with National Centers for Environmental Prediction (NCEP) Global Forecast System (GFS) analysis data for 2001 at an intermediate resolution of T42 (64×128 grid points), with 42 vertical layers. The model is run in a semi-offline mode, relying only on a limited set of input data fields, which are surface pressure, geopotential, temperature, horizontal winds, surface latent and sensible heat fluxes, and zonal and meridional wind stresses. These are interpolated in time to the model time step of 30 min, and used to diagnose transport by advection, vertical diffusion, and deep convection, as well as the tropospheric hydrological cycle (water vapor transport, cloud condensate formation, and precipitation).

For deep convection, MATCH uses two parameterizations called sequentially, following the procedure used in the CCM3 (Kiehl et al. 1996). The penetrative deep convection scheme (Zhang and McFarlane 1995, hereafter ZM95) is based on a reformulation of the PEF of AS74 to a BF, with four main steps: 1) the BF is achieved by analytically solving the equations for an implicit PEF; 2) this analytical solution is facilitated by the simplifying assumptions that the entrainment rate (λ) is constant for each ensemble member, that all updrafts start at the same base level, and that the updraft base mass flux is evenly distributed per increment of λ; 3) the closure assumption is that the base mass flux is scaled so that the convective available potential energy (CAPE) is depleted with a characteristic time constant; and 4) a set of entraining downdrafts is added, all of which detrain air only at the base level of the updrafts. The second convection scheme used in MATCH is from Hack (1994), which is a three-layer convective adjustment scheme that removes any remaining instability after the ZM95 convection. The ZM95 scheme mainly represents deep convection, which is rooted in the BL, while the Hack scheme mainly represents the effects of all other types of convection (shallow moist BL convection plus deeper convection originating above the BL). The results here are shown with the transport by the Hack scheme included. We have also redone the same sensitivity runs without tracer transport by the Hack scheme, which yield the same conclusions and only small quantitative differences (order 1%) from the comparison of the BF with the PEF discussed below.

b. Decomposition of a bulk mass flux vertical profile into a discrete plume ensemble

Comparing a PEF and its corresponding BF approximation can be done in two different ways. One way is to start with an explicit PEF parameterization and simply sum up the plumes into a single bulk plume for the BF transport. The other possibility is to start with a BF parameterization and decompose the bulk plume into individual discrete plumes for use in the PEF transport. Such a decomposition will not necessarily yield a unique set of discrete plumes; thus it is important to check that the decomposition results in a set of plumes that are consistent with the basic assumptions underlying the BF approximation. In either case, only the transport of tracers should be modified to compare the PEF and BF specifically for tracer transport; the treatment of water vapor, moist static energy, precipitation, and other parameters should be kept the same as in the original parameterization so that the overall modeled circulation is not modified.

In this study, we use the BF parameterization by ZM95 as employed in MATCH and the CCM3. ZM95 is based on the plume ensemble concept, but by making use of a few simplifying assumptions (see section 2a), it directly derives the corresponding bulk mass flux profiles. The parameterization does not explicitly compute the mass flux profiles for the discrete plume ensemble members. Thus, we must first decompose the bulk plumes from ZM95 to determine a consistent set of discrete plume ensemble mass flux profiles in each column.

The decomposition of a bulk mass flux profile into its corresponding discrete plume ensemble is in principle straightforward. The mass flux profiles of the discrete ensemble members can be deduced one at a time, starting with the tallest plume. This makes use of two properties of the entraining plume model. First, each discrete plume only detrains in a single model layer. Thus, the mass flux, entrainment flux, and detrainment flux of the tallest plume in the uppermost convective layer are simply equal to the corresponding bulk fluxes in that layer. Second, the entrainment rate (λ) of each plume is assumed to be constant with altitude. This can be used with Eq. (1) (in discrete form) to determine the mass and entrainment fluxes for the tallest plume in each layer below the top, down to the updraft base. These mass flux and entrainment flux vertical profiles for the tallest plume are then subtracted off from the bulk mass and entrainment flux profiles, yielding new bulk profiles in which the uppermost detrainment layer now corresponds to the second tallest discrete plume ensemble member. The same procedure is then repeated recursively for this and each shorter plume until the lowermost detrainment layer has been reached, and the mass flux profiles for each of the discrete plume ensemble members have been determined.

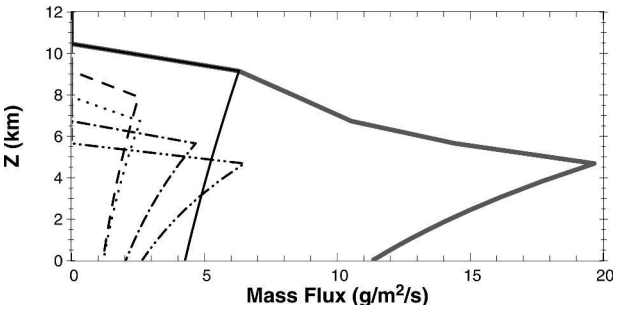

FIG. 2. Sample decomposition of the vertical mass flux profile of a BF plume (thick solid gray line) into its individual discrete PEF members for a model column over central Africa. The thin lines of different types represent each discrete plume, with the thin solid line being the tallest plume and the dash–dot–dot line being the shortest plume.

In practice, a slightly different approach is taken (treating all the plumes in parallel in each model layer starting from the top, rather than decomposing one plume at a time from top to bottom), and a few difficulties are encountered in the application of this approach to the ZM95 parameterization, particularly having to do with the discretization of Eq. (1). These are outlined in the appendix, along with an examination of whether the decomposed plumes are consistent with the basic assumptions in ZM95. It is also worth noting that the decomposition outlined here would also be possible, though more complex, for entraining plume models with a varying λ.

An example of the bulk convective mass flux profile from ZM95 and its decomposition into a set of discrete plume ensemble members is shown in Fig. 2. This example gives an indication of the typical differences in the entrainment rates of the plume ensemble members: at the surface the mass flux of the tallest plume is considerably larger than the mass flux of the shortest plume, while by the time the shortest plume reaches its detrainment layer (~5 km) its mass flux has more than doubled, growing to be greater than the mass flux that the tallest plume attains at its detrainment level (~10 km). The slope of the bulk mass flux (below ~5 km) is between these two extremes, and is clearly much larger than the slope of the tallest plume. Thus, as described in the introduction, the parcels which reach about 8 km or higher in the BF will have been considerably more diluted by air below about 5 km than the parcels reaching the highest detrainment layers of the PEF.

c. Tracer transport algorithms

The transport of tracers based on the bulk and plume ensemble mass fluxes is computed with a new, mass-conserving, monotonic numerical scheme developed for this study, which is in principle similar to the transport algorithms used in previous studies (e.g., Mahowald et al. 1995; Brinkop and Sausen 1997; Rasch et al. 1997), but generalized to allow either PEF or BF transport, and with particular attention to guaranteeing monotonicity for all scenarios (provided the incoming mass fluxes are balanced). The transport is done in three steps, which are largely the same for the PEF and the BF:

1) the mixing ratios in the updrafts are computed for each model layer and each discrete plume (or the single bulk plume) between the updraft base and cloud top in order to determine the mixing ratios in the detraining air masses;
2) the downdraft mixing ratios in each layer and in the air detraining from the downdrafts are determined by repeating this procedure in the opposite direction;
3) the environmental profile of each tracer is updated to reflect the changes due to the convective transport (detrainment from the updrafts and downdrafts and mass-balance subsidence or ascent).

1) UPDRAFTS

The continuity equation for a tracer mixing ratio Q_u (kg kg^{-1}) in an updraft (PEF or BF) is

$$\frac{1}{\rho}\frac{\partial}{\partial z}(F_u Q_u) = E_u Q_{\text{env}} - D_u Q_u, \tag{2}$$

where z is the altitude (m), ρ is the ambient air density (kg m^{-3}), F_u is the updraft mass flux (kg m^{-2} s^{-1}), E_u and D_u are the entrainment and detrainment rates, respectively (s^{-1}), and Q_{env} is the environmental mixing ratio (kg kg^{-1}). The generalized discretization of this for a single model layer is depicted in Fig. 3. For the PEF, for a single plume Eq. (2) becomes

$$F_u^k Q_u^k - F_u^{k+1} Q_u^{k+1} = F_e^k Q_{\text{env}}^k - F_d^k Q_d^k, \tag{3}$$

where the left-hand side represents the vertical discretization of $\partial(F_u Q_u)$, k (superscripted) is the current layer index, $k + 1$ is the layer below the current layer, and Q_d^k is the detraining mixing ratio [described below in Eqs. (6) and (7)]. The entrainment F_e^k and detrainment (F_d^k) terms are expressed in Eq. (3) as mass fluxes (in kg m^{-2} s^{-1}), which are related to the entrainment rates by the hydrostatic equilibrium approximation: $F_e^k = E_u^k \Delta P^k / g$ and $F_d^k = D_u^k \Delta P^k / g$ where ΔP^k is the absolute pressure difference across the layer k, and g is the gravitation constant.

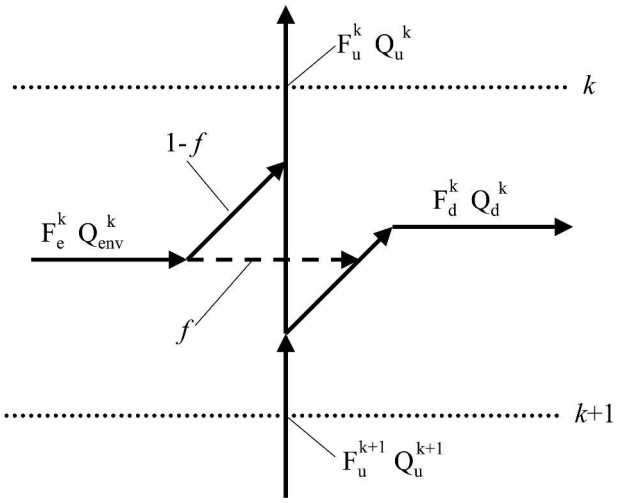

FIG. 3. Schematic of the fluxes F and mixing ratios Q (see text for definitions) in the convective transport algorithm for a single model layer k (generalized to include the f term used in the BF). The layer interfaces are indicated with dotted lines and are labeled k for the top interface and $k + 1$ for the bottom; F_u^k and Q_u^k are interface values leaving the layer, F_u^{k+1} and Q_u^{k+1} are interface values entering the layer from below, while F_e^k, F_d^k, Q_{env}^k, and Q_d^k are average values across the layer.

Rearranging Eq. (3) gives the updraft mixing ratio leaving the top of any nondetraining layer ($F_d^k = 0$) for a single plume in the PEF:

$$Q_u^k = \frac{F_u^{k+1} Q_u^{k+1} + F_e^k Q_{\text{env}}^k}{F_u^k}. \tag{4}$$

Starting at the updraft base level, where the updraft mixing ratio is set equal to the environmental mixing ratio, this is then used recursively to solve for Q_u^k in each convectively active layer k above the updraft base and below the detrainment layer. The implementation of ZM95 in MATCH guarantees that the mass fluxes in any layer k are balanced:

$$F_u^k = F_u^{k+1} + F_e^k - F_d^k. \tag{5}$$

By setting $F_d^k = 0$ in Eq. (5), one sees that the updraft mixing ratio Q_u^k is computed in Eq. (4) as a mass-flux-weighted mean of Q_u^{k+1} and Q_{env}^k, which is an important part of guaranteeing monotonicity in this formulation [also note that for a spatially uniform tracer mixing ratio, Eq. (4) reduces to being the same as Eq. (5), which contributes toward satisfying mass conservation].

For each plume in the PEF, in its detraining layer (where $F_d^k > 0$) the tracer mixing ratio in the detraining air mass (Q_d^k) is determined from the tracer entering the layer from below plus any tracer, which is entrained in

the detraining layer (which can be significant given grid cell depths of the order of a kilometer typical for global models):

$$Q_d^k = \frac{F_u^{k+1}Q_u^{k+1} + F_e^k Q_{\text{env}}^k}{F_d^k} = \frac{(F_d^k - F_e^k)Q_u^{k+1} + F_e^k Q_{\text{env}}^k}{F_d^k}, \quad (6)$$

where the second expression demonstrates monotonicity in the column (i.e., Q_d^k will be between Q_u^{k+1} and Q_{env}^k), and is derived by substituting Eq. (5), noting that $F_u^k = 0$ by definition for the PEF (since all mass detrains in the detraining layer). The detrainment mixing ratio in each plume for the PEF is then used to update the environment in the final step [Eq. (9), below].

For the BF, as for the PEF, Eq. (4) is used to compute Q_u^k in nondetraining layers. However, in contrast to the PEF, in each detraining layer of the BF (except at the cloud top), there is still a mass flux leaving the layer through the top. Some fraction of the air that entrains in a given model layer will continue through to the next layer, while the rest will be entrained into the implicit, infinitesimal plumes that detrain in that layer. The component, which both entrains and detrains in the current layer, is indicated by the dashed lines in Figs. 1b and 3; this fractionation is an artifact due to the reduction of an ensemble of entraining plumes to a single bulk plume on discrete levels, which can be seen in comparison to Fig. 1a. To account for this, an additional term f (the fraction of the air entraining in a layer that detrains in the same layer) is introduced into the equations, so that the detraining mixing ratio for any layer with $F_d^k > 0$ is then computed for the BF as

$$Q_d^k = \frac{(F_d^k - fF_e^k)Q_u^{k+1} + fF_e^k Q_{\text{env}}^k}{F_d^k}, \quad (7)$$

where the form of Eq. (7) is chosen to be mass conserving and monotonic for Q, and can be compared with Eq. (6). Combining this with Eq. (3) gives the updraft mixing ratio

$$Q_u^k = \frac{[F_u^{k+1} - (F_d^k - fF_e^k)]Q_u^{k+1} + (1-f)F_e^k Q_{\text{env}}^k}{F_u^k}, \quad (8)$$

which is comparable to Eq. (4), modified to be applicable to detraining layers in the BF.

The parameter f, which is a consequence of simplifying a PEF to a discrete BF, has not, to our knowledge, been discussed explicitly in the previous literature on convective tracer transport. For thermodynamic aspects of convection, it has not been considered to be a significant issue because air entrained into the updraft is frequently assumed to become saturated immediately at the updraft temperature, based in turn on the assumption that there is nearly always sufficient cloud condensate present to maintain saturation (G. Zhang 2004, personal communication). For tracers, on the other hand, the choice of f can result in significant differences in convective transport, as shown in the results below.

Unfortunately, there are no clear guidelines for choosing an appropriate a priori value or range of values for f, which depend on the characteristics of the entraining plumes in the convection parameterization, as well as on the vertical resolution of the model (for thicker layers, the detraining air mass will represent a greater fraction of the total plume ensemble mass flux, so that f will be larger). The value of f will be different for each model grid cell in which detrainment occurs. The only way to determine a proper value for f for a given grid cell is to go through the decomposition of the bulk mass flux profile described in section 2b, then to compute the ratio of the entrainment flux into the plume that detrains in that layer versus the entrainment flux into the remaining plumes that pass through to higher layers. Doing this for each model column, however, would essentially defeat the purpose of having a simplified bulk formulation. As an alternative, we have collected statistics on the value of f from test runs in which the bulk plumes have each been decomposed. For the month being considered in this study, the global average and standard deviation are $f = 0.33 \pm 0.16$, with values being slightly higher in the extratropics. We have also run tests with the NCEP–National Center for Atmospheric Research (NCAR) 40-yr reanalysis data (Kalnay et al. 1996), which has a lower vertical resolution of only 28 layers (instead of 42 in the GFS analysis), for which we compute a higher value of $f = 0.45 \pm 0.21$, as anticipated. Given the large variability in these diagnosed values of f (with relative standard deviations of about 50%), choosing any particular single value for f, in order to maintain the simplicity of the BF, can only be seen as a rough approximation for all clouds in the BF, and would need to be chosen differently for each new model configuration. Instead, in order to examine the overall importance of this feature of BF convective transport and the choice of f, we test two extreme cases, one with $f = 0.5$ (the upper end of the range of typical values for this configuration of MATCH with ZM95), and the other with $f = 0$. The latter case can be seen as completely neglecting this transport component and instead assuming that the detraining air is comprised only of the air entering from below and that all entrained air joins the mass flux into the next layer, which is likely to

represent what has been done in some of the other BF convective transport schemes currently in use. Because a higher value of f results in less dilution of the air masses that continue on to higher levels, the case with $f = 0.5$ can be expected to give results for the BF (for surface tracers), which are closer to the PEF than the $f = 0$ case.

2) DOWNDRAFTS

In ZM95, downdrafts only detrain in a single layer in each column (which is at the updraft base level), and thus the PEF and BF for downdrafts in ZM95 reduce to being identical (this is not necessarily the case for other bulk convection schemes). The same procedure as the BF updrafts is thus used based on the downdraft mass fluxes and entrainment fluxes, initializing the downdrafts with the preconvection environmental mixing ratios from the respective layers, to determine the tracer mixing ratios in the air that finally detrains from the downdrafts. Note that in the next section, the treatment is generalized to allow either PEF or BF downdrafts.

3) UPDATING THE ENVIRONMENTAL MIXING RATIOS

The final step is to update the environment to reflect the changes due to the convective transport, which is computed for a given model layer as

$$Q^k_{\text{env}}(t + \Delta t) = \frac{\left[\sum_{i=1}^{N_u} F^k_d(i) Q^k_d(i) + \sum_{i=1}^{N_d} F^k_{\text{dd}}(i) Q^k_{\text{dd}}(i) + F^k_s Q^{k-1}_{\text{env}}(t)\right]\Delta t + M^k_r Q^k_{\text{env}}(t)}{M^k}, \tag{9}$$

where t is the time and Δt is the time step (s), N_u and N_d are the number of updraft and downdraft plumes, respectively, F_{dd} is the detrainment flux from downdrafts (kg m^{-2} s^{-1}, taken to be positive), Q^k_{dd} is the tracer mixing ratio in the detraining air from the downdrafts (kg kg^{-1}), and M^k is the column mass density (kg m^{-2}) of the grid cell ($M^k = \Delta P^k/g$), F^k_s is the downward air-mass flux due to subsidence (kg m^{-2} s^{-1}), which balances the difference in the updraft and downdraft mass fluxes (note that in ZM95 the updraft mass flux is always larger than the downdraft), computed as

$$F^k_s = \sum_{i=1}^{N_u} F^k_u(i) - \sum_{i=1}^{N_d} F^k_{\text{down}}(i), \tag{10}$$

where $F^k_{\text{down}}(i)$ is the downdraft mass flux of plume i at the interface k, and M^k_r is the residual air mass left in the cell

$$M^k_r = M^k - \left[\sum_{i=1}^{N_u} F^k_d(i) + \sum_{i=1}^{N_d} F^k_{\text{dd}}(i) + F^k_s\right]\Delta t. \tag{11}$$

Thus, the first and second terms in the numerator on the right-hand side in Eq. (9) are the amounts of the tracer added to the environment by the full set of N_u updrafts and N_d downdrafts, respectively (for the BF, $N_u \equiv N_d \equiv 1$, and generally for downdrafts in ZM95, $N_d \equiv 1$), the third term is the tracer added from the layer above due to mass balance subsidence, and the fourth term is the tracer left over in the grid cell from before the convective redistribution. Chemical changes (e.g., decay) during the convective transport are neglected. Although the simple upwind differencing approach used in Eq. (9) is known to result in numerical diffusion (e.g., Rood 1987), it has been chosen for use here as a straightforward final step in guaranteeing mass conservation and monotonicity.

Finally, it is important to note that the difference between the BF and the PEF is not simply a consequence of the discretization (even if a higher order discretization or vertical resolution were used). The difference arises in the computation of the tracer mixing ratio in the updraft in Eq. (8) (where $f \equiv 0$ for the PEF). In a nondetraining layer, where $F^k_d = 0$ and thus $f = 0$ also for the BF, this reduces to Eq. (4) for both the PEF and BF, in which the fraction F^k_e/F^k_u determines the dilution of the convective core mixing ratio (Q_u) with environmental air (Q_{env}). This fraction is related to λ [Eq. (1)], and is thus larger for the BF than for the tallest plumes in the PEF. Thus, by the time the first detraining layer is reached, Q_{env} contributes more to Q_u in the BF than in the tallest plumes of the PEF. This difference holds regardless of how many layers are used or how short the time step is. The introduction of the parameter f, which as discussed above can be approximated based on information from the decomposition of the bulk plume into a discrete ensemble, helps to reduce the difference between the BF and PEF, but only in the detraining region of the convective column.

d. Runs

The runs examined in this study focus on insoluble tracers with uniform surface emissions of 10^{-11} kg m^{-2} s^{-1} and a constant radioactive like decay in the atmo-

sphere, with *e*-folding lifetimes of 0.5, 1, 2, 5, and 10 days. This suite of tracers gives information that is relevant for a wide range of actual gases in the atmosphere with predominantly surface or lower tropospheric sources, such as radon, dimethylsulfide (CH_3SCH_3), CH_3I, nitrogen oxides ($NO_x = NO + NO_2$), CH_3OOH, and isoprene (C_5H_8). The effects on real gases in full atmospheric chemistry simulations will be examined in follow-up studies, after the new transport scheme is extended to consider the effects of precipitation scavenging. Three runs are examined here with this set of tracers: 1) PLUME, using the profile decomposition described in section 2b and the PEF transport algorithm in section 2c; 2) BULK, using the original bulk mass flux profiles from the ZM95 scheme with the tracer transport scheme in section 2c, and with $f = 0.5$; and 3) BULK-0, which is like the BULK run but with $f = 0$. The runs are started in June 2001, and given one month for the tracer distribution fields to spin up from their initial mixing ratio of zero everywhere; model output is examined for July 2001. In all of the runs, only the transport of the chemical tracers is modified; tendencies for water and potential temperature due to convective transport are computed internally by the ZM95 parameterization and are left unchanged between the runs, so that the bulk mass fluxes and other aspects of the simulated meteorology (e.g., the tropospheric hydrological cycle) are the same for all runs.

3. Effects of the transport formulation on short-lived tracers with surface sources

The zonal mean distributions of the tracers with $\tau =$ 1 day and $\tau = 2$ days for the PLUME run (Figs. 4a,b) reflect the general tendency of the modeled deep convection to be strongest in the Tropics, and to detrain in a broad region covering the middle and upper troposphere, resulting in a local minimum in the mixing ratios in the lower troposphere. These c-shaped vertical profiles are commonly observed for reactive trace gases in the troposphere. For these short-lived tracers, the mean mixing ratios decrease very rapidly above the tropopause.

The relative differences of these tracers in the PLUME versus the BULK run (Figs. 4c,d) show that, as expected from the discussion above, using the PEF enhances the transport of a surface tracer to the highest layers compared to using the BF, and reduces the transport to the lower and middle troposphere. Monthly zonal mean differences exceed 20% of the BULK run value for the $\tau = 1$ day tracer throughout most of the tropical tropopause layer (TTL), overlapping with the top of the simulated primary convective outflow region (Fig. 4a), while the differences are smaller (<15%) in the extratropical UT. The differences are larger for shorter-lived tracers and smaller for longer-lived tracers. They are also significantly larger if the BF neglects the detrainment of air that has entrained in the same model layer (i.e., the BULK-0 run), as shown in Figs. 4e,f. In this case, the difference in efficiency of transport of short-lived tracers to the top of the TTL reaches 50% in the zonal, monthly mean, and can exceed 20% in the summertime extratropical UT.

A summary of the results in terms of the tracer masses in the UT in the three sensitivity runs is given in Table 1. The difference in the mean transport to the UT between the PLUME and BULK runs is about twice as large in the Tropics as in the extratropics. For the very short-lived surface tracers, the PLUME run computes monthly mean masses of the tracers in the tropical UT which are up to 22% higher than in the BULK run, while for tracers with $\tau \geq 5$ days the difference between the two runs is less than 10%. The differences between the PLUME and BULK-0 runs are about half again as large as the differences between the PLUME and BULK runs. Since the use of $f = 0.5$ in the BULK run mainly reduces the differences in the detrainment region, this indicates that most of the total difference between the PLUME and BULK-0 runs is due to entrainment in the nondetraining layers. Recall that our choice of the test value of $f = 0.5$ is at the high end of the range we diagnosed as being typical for this model configuration. This should not only reduce the differences in the detraining region (for surface tracers), but will also help to compensate for some of the difference below the detraining region; nevertheless, even this is far from being able to fully alleviate the differences between the PEF and BF.

Much larger differences can be expected on shorter time scales during intense convective activity. In regions of strong convective outflow, UT tracer mixing ratios in the PLUME run can exceed those in the BULK run by more than a factor of 2 (based on 3-h average model output); example profiles showing such differences are plotted in Fig. 5. In the uppermost regions of convective outflow, where the mass flux is decreasing rapidly with height, the differences for individual profiles can exceed an order of magnitude. For atmospheric chemistry, especially for comparisons to field observations, it is important to know how frequent these large differences are. Figure 6 shows the cumulative frequency distribution of the relative differences between individual profiles from the PLUME and BULK runs. If one only considers layers with strong convective outflow (Fig. 6a), which can only be produced if dilution with midtropospheric air (which erodes the buoyancy) is limited, differences of >10%

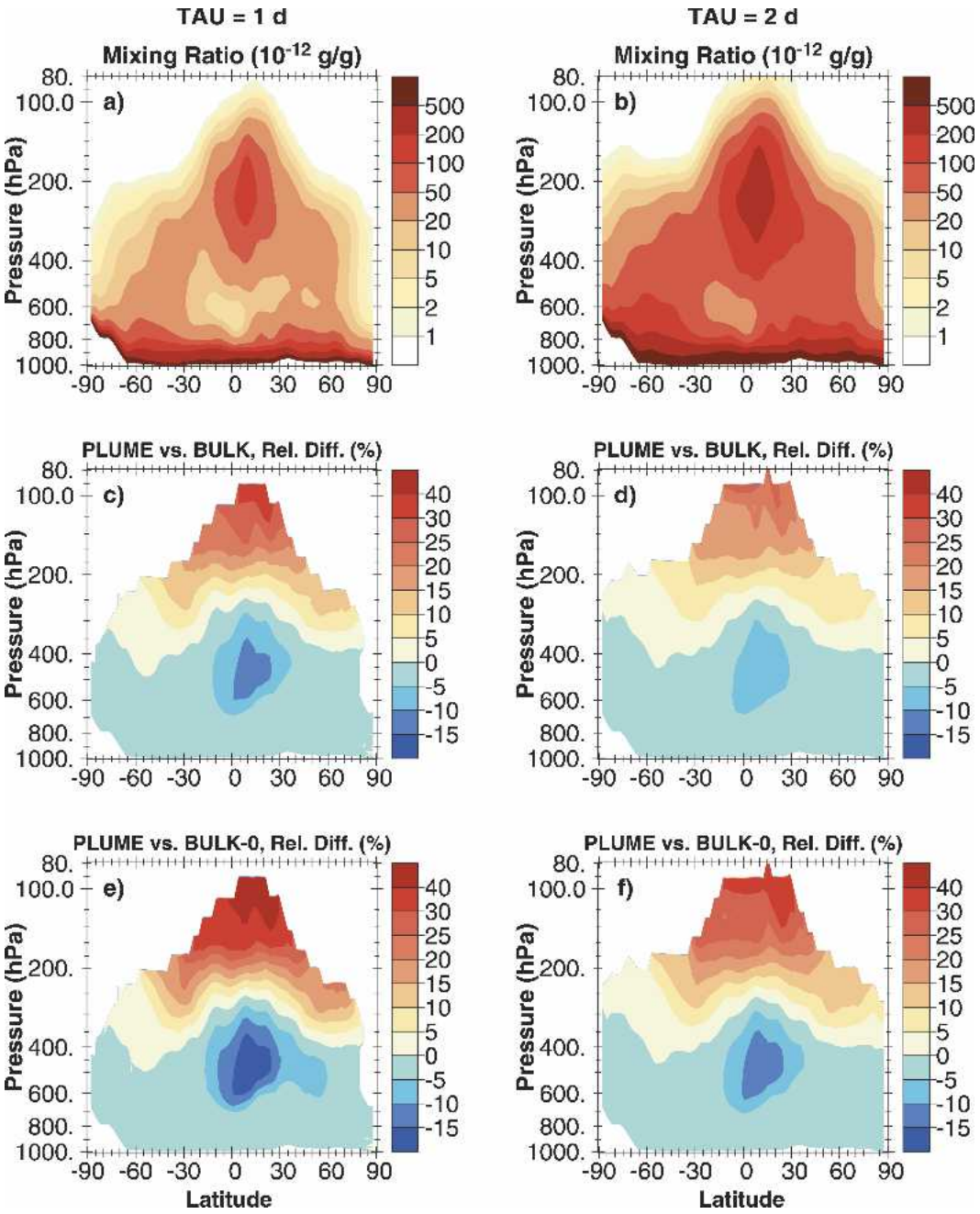

FIG. 4. Results for the (left) $\tau = 1$ day and (right) $\tau = 2$ day tracers for Jul 2001: (a), (b) zonal mean mixing ratio distributions (in 10^{-12} g g^{-1}); (c), (d) relative differences of the zonal mean distributions from the PLUME vs BULK runs—computed as 100[(PLUME − BULK)/BULK]; (e), (f) relative differences of the zonal mean distributions from the PLUME vs BULK-0 runs—100[(PLUME − BULK-0)/BULK-0]. The ratios are only plotted for model layers in which the zonal mean mixing ratio of the tracer in the PLUME run is $>10^{-3}$ of the zonal mean mixing ratio in the underlying model surface layer.

between the tracers in the PLUME and BULK runs can nevertheless be found in more than half of the convective columns, except for the $\tau = 10$ day tracer, and differences exceeding 30% are common for the shorter-lived tracers. If the criterion is relaxed to columns with moderate convective outflow (Fig. 6b), larger differences become more frequent. In this case, for the very short-lived tracers ($\tau \leq 2$ days), differences of more than 50% can be found in more than 1% of the profiles, and even for the $\tau = 5$ day tracer, the differences ex-

TABLE 1. Tracer masses (10^6 kg) in the sensitivity runs for the tropical and extratropical UT.

Tau (days)	PLUME (10^6 kg)	BULK (10^6 kg)	PLUME vs BULK[a] relative difference (%)	BULK-0 (10^6 kg)	PLUME vs BULK-0[a] relative difference (%)
Tropical UT[b]					
0.5	0.284	0.232	22.4	0.209	35.9
1.0	0.832	0.699	19.0	0.644	29.2
2.0	2.280	1.980	15.2	1.870	21.9
5.0	7.560	6.880	9.9	6.640	13.9
10.0	16.900	15.900	6.3	15.500	9.0
Extratropical UT[c]					
0.5	0.163	0.147	10.9	0.139	17.3
1.0	0.501	0.463	8.2	0.443	13.1
2.0	1.520	1.430	6.3	1.380	10.1
5.0	6.320	6.060	4.3	5.940	6.4
10.0	17.100	16.600	3.0	16.300	4.9

[a] Relative difference due to using a PEF vs using a BF with $f = 0.5$ or $f = 0.0$, computed as [100 (PLUME − BULK)/BULK] or [100 (PLUME − BULK-0)/BULK-0], respectively.
[b] 30°S–30°N, above 200 hPa.
[c] 90°–30°S plus 30°–90°N, above 300 hPa.

ceed 20% more than 14% of the time. On the other hand, for longer-lived tracers ($\tau \geq 10$ days), the differences between the PLUME and BULK runs are generally small, rarely exceeding 20%.

Finally, we have also examined simple tracers with sources in other vertical regions, which for brevity have not been included in detail here. The differences between the PEF and BF are typically largest for tracers with midtropospheric sources. In this case, the main pathway for the tracers to reach the UT is via midtropospheric entrainment, and thus (in contrast to surface tracers) the BF strongly overestimates the efficiency of vertical transport of these tracers relative to the PEF.

4. Implications for atmospheric chemistry simulations

Although follow-up studies on the impact of PEF versus BF transport on real reactive gases and aerosols (e.g., ozone and sulfate) will first require the development of a new precipitation scavenging algorithm consistent with the transport algorithm presented here, a few implications, especially for O_3-related gas phase atmospheric chemistry, can already be anticipated. First, convective transport of short-lived gases provides a significant source of HO_x (=OH + HO_2) to the UT (e.g., Prather and Jacob 1997; Jaeglé et al. 2001), which determines the UT oxidizing efficiency, and in turn influences the lifetimes of radiatively active gases such as CH_4. Our results suggest that very short-lived gases likely have an even more important role for the UT HO_x budget than found in previous simulations, most of which were done with chemistry transport models (CTMs) using BF transport parameterizations (e.g., Collins et al. 1999). This may especially be the case for CH_3OOH, since its lifetime is less than a day, and the primary region where it can compete with other main HO_x sources is near the tropopause, where we compute the largest increase in the efficiency of transport with the PEF versus BF.

Similarly, NO_x (=NO + NO_2), which has a lifetime of about a day in the lower troposphere, will also be more efficiently transported to the UT by the PEF than by a corresponding BF. Convective transport of NO_x tends to increase global levels of O_3, an important greenhouse gas, since in the UT the NO_x lifetime is longer, and its O_3 production efficiency is greater than near the surface (e.g., Dickerson et al. 1987; Pickering et al. 1990; Lawrence et al. 2003a). Determining whether this can compete with the source of NO_x from lightning, however, will require runs with a global CTM.

Finally, comparisons of model output with vertical profile measurements are expected to be affected for tracers with large vertical gradients in convectively active regions, as demonstrated in Fig. 5. Much of the past work in evaluating CTMs with observations has focused on climatological values (e.g., monthly means) of trace gases (Hauglustaine et al. 1998; Lawrence et al. 1999a; Bey et al. 2001; Horowitz et al. 2003; and others). For MATCH we have noted that UT mixing ratios of several trace gases with primarily lower tropospheric sources, such as CO, C_2H_6, C_4H_8, C_2H_6, CH_2O, and NO are often underestimated in convective, polluted regions [see the figures for the regions PEM-West-A: China-Coast-E, TRACE A: Brazil-E, TRACE A: Africa-S, and TRACE A: Africa-Coast-W in von Kuhl-

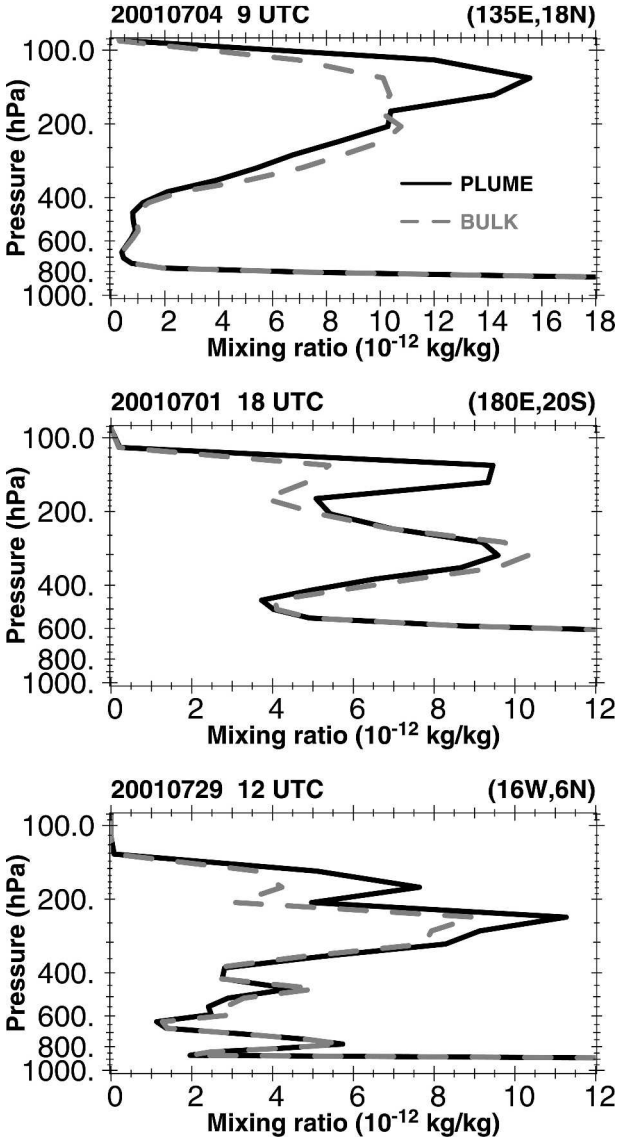

FIG. 5. Sample vertical profiles of the tracer mixing ratios for the $\tau = 1$ day tracers (3-h average output) for the three date–times indicated showing the differences between the PLUME and BULK runs in regions of strong convective outflow.

mann et al. (2003b)]. The more efficient PEF transport may help to reduce some of these discrepancies; however, because of the very large number of other uncertainties that could also influence the vertical profiles, such as the overall convective mass fluxes, upper tropospheric oxidation rates, and scavenging of soluble intermediates, along with sampling issues of comparing point measurements with model results, it is currently not possible to make use of observations to critically evaluate the BF and PEF transport formulations. In addition to these climatological studies, recently we have begun using MATCH to analyze individual vertical profiles of trace gases from a number of different field campaigns (e.g., Lawrence et al. 1999a, 2003b; Lawrence 2001). Furthermore, MATCH and many other models are now being used to make short-term chemical weather forecasts for guiding field campaign flights (e.g., Lawrence et al. 2003b). Such analyses and forecasts will be sensitive to various uncertainties in the parameterization of deep convection, including the treatment of tracer transport, for example, with an explicit PEF or a corresponding BF simplification.

5. Conclusions

This study contributes toward our understanding of the effects of deep convection on tropospheric tracers and the sensitivity of chemistry transport model simulations to the characteristics of convective transport parameterizations. Previous studies (Mahowald et al. 1995; Collins et al. 2002) have compared different convection schemes in 1D and 3D models and showed that they can lead to substantial differences in the vertical distributions of various short-lived tracers. In this study, we have shown that even for a single convection parameterization (ZM95), significant differences in the UT mixing ratios of short-lived tracers can result, depending on how the convective mass fluxes are computed and applied to tracer transport. This applies not only to the difference between the PEF versus BF treatments of tracer transport, but also to the implementation of the entrainment and detrainment fluxes within the BF itself (i.e., the notable differences between the BULK and BULK-0 cases, which can be seen implicitly in Fig. 4).

The differences resulting from simplifying a PEF to a BF depend on the lifetime (τ) of the tracer in question. For $\tau \gtrsim 5$ days, the use of a simplified BF appears to be justified for simulations of surface tracers, particularly when monthly mean output is being examined. On the other hand, for shorter-lived ($\tau \lesssim 2$ days) surface tracers, or more generally for any tracer with a strong vertical gradient prior to the occurrence of deep convection, the reduced efficiency in the amount of tracer transported to the UT resulting from the use of the BF can be significant, exceeding 30% in the zonal mean averaged over a month in our simulations, and even greater on shorter time scales.

Future studies of the effects of deep convection on tropospheric gas and aerosol chemistry are still needed to address several issues. In particular, in order to apply the transport algorithm developed here to "real" tropospheric chemistry, it will need to be extended to account for the uptake of soluble gases and aerosols in

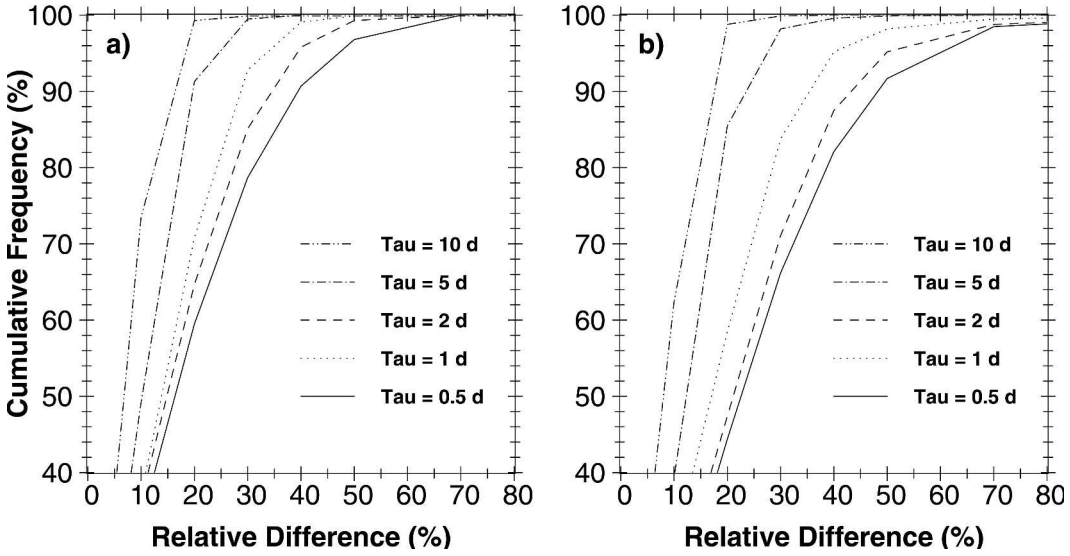

FIG. 6. Cumulative frequency distributions of the relative differences between the PLUME and BULK runs for different taus (τ). The frequencies are computed for the maximum relative difference 100[(PLUME − BULK)/BULK] in each model column above 500 hPa, based on 3-h average output, in columns with active convection: (a) only considering layers with strong convective outflow, where the mixing ratio in that layer (for the PLUME run) exceeds 10% of the global average surface mixing ratio; (b) considering layers with moderate convective outflow, with at least 1% of the global average surface mixing ratio. Only the upper portion of the cumulative frequency distribution is plotted to better distinguish the curves. The values are computed for bins with a width of 10% relative difference, and are plotted so that each point shows the frequency of occurrence of that or a smaller relative difference.

hydrometeors in the updrafts and downdrafts. We are currently working on taking advantage of the more detailed formulation of tracer transport developed here as a foundation for advancing beyond the current state of the art in convective scavenging schemes (e.g., Roelofs and Lelieveld 1995; Crutzen and Lawrence 2000; Liao et al. 2003).

This study has given a further example of the value of tracers in analyzing the differences in various approaches to parameterizing convection. Besides comparing different convection schemes (Mahowald et al. 1995; Collins et al. 2002), or comparing different transport algorithms for one scheme (as done here), it would also be valuable to examine the sensitivity to systematically varying parameter choices within a single parameterization. To our knowledge, such a study for tracers has not yet been published. Key parameters to examine would include CAPE thresholds for triggering convection, alternative closure assumptions (e.g., Zhang 2002, 2003; Donner and Phillips 2003), and the partitioning of convective mass fluxes among plume ensemble members. The latter parameter is particularly relevant to our comparison of the PEF and BF. The largest differences between the PEF and BF for surface tracers is expected to be found when the base mass flux distribution is biased toward shallower clouds, since this will cause a greater dilution with midtropospheric air for the parcels reaching the highest levels in the BF. The smallest differences will be when most of the base mass flux goes into the tallest cloud elements. The choice in ZM95 can be seen as intermediate: the mass flux is partitioned evenly as a function of the entrainment rate (λ, which determines the height of each cloud element). This was indicated by ZM95 to be a relatively arbitrary choice, motivated mainly by the fact that it allows an analytical solution to reduce the implicit PEF to a BF. Determining an optimal partitioning for use with a PEF is a major outstanding research need, requiring further theoretical studies, targeted observations, and cloud resolving model simulations.

Finally, in addition to these comparisons of the PEF and BF for tracer transport, it may be worthwhile to revisit the comparison for thermodynamic quantities, particularly in the framework of schemes that are either widely used or are currently under development for future use. Furthermore, it would be interesting to repeat the comparisons done here from the opposite approach of beginning with an explicit PEF scheme and combining the mass flux profiles to allow the transport with a corresponding BF to be tested. This would be particularly enlightening with some of the more recent developments in explicit PEF parameterizations (e.g.,

Donner et al. 2001; Nober and Graf 2004). Generally, this research on explicit PEF schemes can be expected to be beneficial for simulations of short-lived tracers, as demonstrated here. As an intermediate alternative, for models that are currently employing BF parameterizations such as ZM95, we have shown that the bulk mass flux profiles can be consistently decomposed into discrete plume ensembles and then used for PEF transport. For the simple tracer simulations done here, the computational expense of this is reasonable, amounting to about 1% additional total run time.

The convective transport routine and bulk plume decomposition algorithm are available for testing and use in other models, and have been successfully implemented (BF only) for test purposes in the ECHAM chemistry GCM (H. Tost and P. Jöckel 2004, personal communication). A version of our code that is well-commented and with a simple interface and switches for easily choosing between the BF or PEF, along with a set of test exercises, can be obtained on request from the lead author, or via http://www.mpch-mainz.mpg.de/~lawrence/conv_plume_transport_code.tar.gz.

Acknowledgments. We appreciate valuable discussions on this topic with many colleagues, especially Marc Salzmann, Guang Zhang, Holger Tost, Leo Donner, Chien Wang, Sabine Brinkop, and Rolf von Kuhlmann. Very thorough reviews from Jun-Ichi Yano and two anonymous referees helped improve and focus the manuscript substantially. This work was supported by funding from the German Ministry of Education and Research (BMBF), Project 07-ATC-02, and in part from the EU FW5 project PHOENICS.

APPENDIX

Practical Issues in the Bulk Plume Decomposition for the ZM95 Parameterization

There are three key difficulties in the application of the bulk plume decomposition to ZM95. The most important is due to the discretization of the spectral plume ensemble into a set of subensembles that are treated on model layers. Because of this, the use of Eq. (1) to determine the mass flux profiles starting at the top of the plume and working down to the updraft base for each discrete ensemble member is not exact. Thus, in each nondetraining layer, the sum of the mass fluxes of the discrete plumes does not add up to the original bulk mass flux in that layer; the difference, however, tends to be small, typically $<1\%$ for adjacent layers. This inconsistency is removed by normalizing the fluxes in each layer, keeping the same relationship between the plumes, so that the plumes always sum to the bulk mass flux profile.

A second difficulty is in diagnosing the entrainment rate of the tallest plume accurately because ZM95, as implemented in MATCH, does not allow entrainment in the uppermost layer of the bulk plume, but does allow both of the two tallest plumes to entrain in the next layer below. This is dealt with by estimating the partitioning of the entrainment between these two plumes based on their detrainment mass fluxes and the properties of the implicit plume ensemble in ZM95 mentioned in section 2a, which only results in a small error (on average less than 10%) in the partitioning at the updraft base for the tallest two plumes (this does not affect the other plumes; this error could be further reduced by iterating up and down the column, but this was not deemed worthy of the extra complexity for this study).

Finally, in rare cases, ZM95 computes a very weak implicit discrete plume ensemble member, where the plume detrainment flux is smaller than the error in the first-order discretization used for Eq. (1). This is dealt with by either adjusting the entrainment fluxes of the other plumes (normally by $<1\%$) so that λ for the weak plume falls between the values for the next taller and shorter plumes, or by simply removing the weak plume from the ensemble by attributing its mass fluxes to the next taller and shorter plumes (done only when the detrainment flux of the weak plume is $<0.1\%$ of the maximum detrainment flux in any taller plume).

The application of this procedure to ZM95 produces a set of discrete plumes whose sum add up exactly to the bulk mass flux profile. An important test of the decomposition is whether the base mass fluxes of the plume ensemble are consistent with the ZM95 assumption of an even distribution of the base mass flux per increment of λ. The entrainment rates λ for the set of discrete plumes are actually not computed in the course of the decomposition; instead, Eq. (1) is only used to equate the ratio of entrainment fluxes and mass fluxes for two vertically adjacent layers. For the sake of the check on the decomposed base mass fluxes, λ is diagnosed for the layer above the updraft base layer using the second-order discretization,

$$\lambda = \frac{1}{(F_u^k + F_u^{k+1})/2} \frac{F_e^k}{\Delta z^k}.$$

It turns out that the decomposition outlined above yields a set of plumes that are already in reasonable agreement with this assumption, with on average less than a 10% deviation from the expected linear relationship between the entrainment rates and cumulative mass fluxes of each of the ensemble members. Because

of the quality of this agreement, further iterations to improve the solution by making small adjustments to the relative plume entrainment rates have not been done for this study.

REFERENCES

Allen, D. J., R. B. Rood, A. M. Thompson, and R. D. Hudson, 1996: Three-dimensional radon 222 calculations using assimilated meteorological data and a convective mixing algorithm. *J. Geophys. Res.,* **101,** 6871–6881.

Arakawa, A., and W. H. Schubert, 1974: Interaction of a cumulus cloud ensemble with the large-scale environment, Part I. *J. Atmos. Sci.,* **31,** 674–701.

Bechtold, P., and Coauthors, 2000: A GCSS model intercomparison for a tropical squall line observed during TOGA-COARE. II: Intercomparison of single-column models and a cloud-resolving model. *Quart. J. Roy. Meteor. Soc.,* **126,** 823–863.

Bell, N., and Coauthors, 2002: Methyl iodide: Atmospheric budget and use as a tracer of marine convection in global models. *J. Geophys. Res.,* **107,** 4340, doi:10.1029/2001JD001151.

Bey, I., and Coauthors, 2001: Global modeling of tropospheric chemistry with assimilated meteorology: Model description and evaluation. *J. Geophys. Res.,* **106,** 23 073–23 095.

Bougeault, P., 1985: A simple parameterization of the large-scale effects of cumulus convection. *Mon. Wea. Rev.,* **113,** 2108–2121.

Brinkop, S., and R. Sausen, 1997: A finite difference approximation for convective transports which maintains positive tracer concentrations. *Beitr. Phys. Atmos.,* **70,** 245–248.

Chatfield, R. B., and P. J. Crutzen, 1984: Sulfur dioxide in remote oceanic air: Cloud transport of reactive precursors. *J. Geophys. Res.,* **89,** 7111–7132.

Collins, W. J., D. S. Stevenson, C. E. Johnson, and R. G. Derwent, 1999: Role of convection in determining the budget of odd hydrogen in the upper troposphere. *J. Geophys. Res.,* **104,** 26 927–26 941.

——, R. G. Derwent, C. E. Johnson, D. S. Stevenson, 2002: A comparison of two schemes for the convective transport of chemical species in a Lagrangian global chemistry model. *Quart. J. Roy. Meteor. Soc.,* **128,** 991–1009.

Crutzen, P. J., and M. G. Lawrence, 2000: The impact of precipitation scavenging on the transport of trace gases: A 3-dimensional model sensitivity study. *J. Atmos. Chem.,* **37,** 81–112.

Dickerson, R. R., and Coauthors, 1987: Thunderstorms: An important mechanism in the transport of air pollutants. *Science,* **235,** 460–465.

Donner, L. J., and V. T. Phillips, 2003: Boundary layer control on convective available potential energy: Implications for cumulus parameterization. *J. Geophys. Res.,* **108,** 4701, doi:10.1029/2003JD003773.

——, C. J. Seman, and R. S. Hemler, 2001: A cumulus parameterization including mass fluxes, convective vertical velocities, and mesoscale effects: Thermodynamic and hydrological aspects in a general circulation model. *J. Climate,* **14,** 3444–3463.

Emanuel, K. A., and M. Zivkovic-Rothman, 1999: Development and evaluation of a convection scheme for use in climate models. *J. Atmos. Sci.,* **56,** 1766–1782.

Gregory, D., and P. R. Rowntree, 1990: A mass flux convection scheme with representation of cloud ensemble characteristics and stability-dependent closure. *Mon. Wea. Rev.,* **118,** 1483–1506.

Grell, G. A., 1993: Prognostic evaluation of assumptions used by cumulus parameterizations. *Mon. Wea. Rev.,* **121,** 764–787.

Hack, J. J., 1994: Parameterization of moist convection in the National Center for Atmospheric Research community climate model (CCM2). *J. Geophys. Res.,* **99,** 5551–5568.

——, W. H. Schubert, and P. L. S. Dias, 1984: A spectral cumulus parameterization for use in numerical models of the tropical atmosphere. *Mon. Wea. Rev.,* **112,** 704–716.

Hauglustaine, D. A., G. P. Brasseur, S. Walters, P. J. Rasch, J.-F. Mueller, L. K. Emmons, and M. A. Carroll, 1998: MOZART, a global chemical transport model for ozone and related chemical tracers, 2: Model results and evaluation. *J. Geophys. Res.,* **103,** 28 291–28 335.

Heimann, M., 1995: The global atmospheric tracer model TM2. Tech. Rep. 10, Deutsches Klimarechenzentrum, Hamburg, Germany, 53 pp.

Horowitz, L. W., and Coauthors, 2003: A global simulation of tropospheric ozone and related tracers: Description and evaluation of MOZART, version 2. *J. Geophys. Res.,* **108,** 4784, doi:10.1029/2002JD002853.

Jaeglé, L., D. J. Jacob, W. H. Brune, and P. O. Wennberg, 2001: Chemistry of HO_x radicals in the upper troposphere. *Atmos. Environ.,* **35,** 469–489.

Kain, J. S., and J. M. Fritsch, 1990: A one-dimensional entraining/detraining plume model and its application in convective parameterization. *J. Atmos. Sci.,* **47,** 2784–2802.

Kalnay, E., and Coauthors, 1996: The NCEP/NCAR 40-Year Reanalysis Project. *Bull. Amer. Meteor. Soc.,* **77,** 437–471.

Kiehl, J. T., G. B. Bonan, B. A. Boville, B. P. Briegleb, D. L. Williamson, and P. J. Rasch, 1996: Description of the NCAR community climate model (CCM3). NCAR Tech. Note NCAR/TN-420+STR, National Center for Atmospheric Research, Boulder, CO, 152 pp.

Kuo, H. L., 1965: On formation and intensification of tropical cyclones through latent heat release by cumulus convection. *J. Atmos. Sci.,* **22,** 40–63.

Lawrence, M. G., 2001: Evaluating trace gas sampling strategies with assistance from a global 3D photochemical model: Case studies for CEPEX and NARE O_3 profiles. *Tellus,* **53B,** 22–39.

——, P. J. Crutzen, and P. J. Rasch, 1999a: Analysis of the CEPEX ozone data using a 3D chemistry–meteorology model. *Quart. J. Roy. Meteor. Soc.,* **125,** 2987–3009.

——, ——, ——, B. E. Eaton, and N. M. Mahowald, 1999b: A model for studies of tropospheric photochemistry: Description, global distributions, and evaluation. *J. Geophys. Res.,* **104,** 26 245–26 277.

——, R. von Kuhlmann, M. Salzmann, and P. J. Rasch, 2003a: The balance of effects of deep convective mixing on tropospheric ozone. *Geophys. Res. Lett.,* **30,** 1940, doi:10.1029/2003GL017644.

——, and Coauthors, 2003b: Global chemical weather forecasts for field campaign planning: Predictions and observations of large-scale features during MINOS, CONTRACE, and INDOEX. *Atmos. Chem. Phys.,* **3,** 267–289.

Lelieveld, J., and P. J. Crutzen, 1994: Role of deep cloud convection in the ozone budget of the troposphere. *Science,* **264,** 1759–1761.

Liao, H., P. J. Adams, S. H. Chung, J. H. Seinfield, L. J. Mickley, and D. J. Jacob, 2003: Interactions between tropospheric

chemistry and aerosols in a unified general circulation model. *J. Geophys. Res.,* **108,** 4001, doi:10.1029/2001JD001260.

Lord, S. J., W. C. Chao, and A. Arakawa, 1982: Interaction of a cumulus cloud ensemble with the large-scale environment. Part IV: The discrete model. *J. Atmos. Sci.,* **39,** 104–112.

Mahowald, N. M., P. J. Rasch, and R. G. Prinn, 1995: Cumulus parameterizations in chemical transport models. *J. Geophys. Res.,* **100,** 26 173–26 189.

——, ——, B. E. Eaton, S. Whittlestone, and R. G. Prinn, 1997a: Transport of ^{222}radon to the remote troposphere using the model of atmospheric transport and chemistry and assimilated winds from ECMWF and the National Centers for Environmental Prediction/NCAR. *J. Geophys. Res.,* **102,** 28 139–28 152.

——, ——, and R. G. Prinn, 1997b: Deducing CCl_3F emissions using an inverse method and chemical transport models with assimilated winds. *J. Geophys. Res.,* **102,** 28 153–28 168.

Manabe, S., J. Smagorinsky, and R. F. Strickler, 1965: Simulated climatology of a general circulation model with a hydrological cycle. *Mon. Wea. Rev.,* **93,** 769–798.

Mari, C., D. J. Jacob, and P. Bechtold, 2000: Transport and scavenging of soluble gases in a deep convective cloud. *J. Geophys. Res.,* **105,** 22 255–22 267.

Moorthi, S., and M. J. Suarez, 1992: Relaxed Arakawa–Schubert—A parameterization of moist convection for general-circulation models. *Mon. Wea. Rev.,* **120,** 978–1002.

Nober, F. J., and H. F. Graf, 2004: A new convective cloud field model based on principles of self-organisation. *Atmos. Chem. Phys. Discuss.,* **4,** 3669–3698.

Pan, H., and W. Wu, 1995: Implementing a mass flux convection parameterization package for the NMC medium-range forecast model. Tech. Rep. 409, U.S. Department of Commerce, National Oceanic and Atmospheric Administration, National Weather Service, National Meteorological Center, 41 pp.

Pickering, K. E., A. M. Thompson, R. R. Dickerson, W. T. Luke, D. P. McNamara, J. P. Greenberg, and P. R. Zimmerman, 1990: Model calculations of tropospheric ozone production potential following observed convective events. *J. Geophys. Res.,* **95,** 14 049–14 062.

——, J. R. Scala, A. M. Thompson, W. Tao, and J. Simpson, 1992: A regional estimate of convective transport of CO from biomass burning. *Geophys. Res. Lett.,* **19,** 289–292.

Prather, M. J., and D. J. Jacob, 1997: A persistent imbalance in HO_x and NO_x photochemistry of the upper troposphere driven by deep tropical convection. *Geophys. Res. Lett.,* **24,** 3189–3192.

Rasch, P., N. M. Mahowald, and B. E. Eaton, 1997: Representations of transport, convection and the hydrologic cycle in chemical transport models: Implications for the modeling of short lived and soluble species. *J. Geophys. Res.,* **102,** 28 127–28 138.

——, D. Zurovac-Jevtic, K. Emanuel, and M. Lawrence, 2003: Consistent representation of convective processes for chemistry and climate models. *Geophys. Res. Abstr.,* **5,** 12 440.

Roeckner, E., L. Bengtsson, J. Feichter, J. Lelieveld, and H. Rodhe, 1999: Transient climate change simulations with a coupled atmosphere–ocean GCM including the tropospheric sulfur cycle. *J. Climate,* **12,** 3004–3032.

Roelofs, G., and J. Lelieveld, 1995: Distribution and budget of O_3 in the troposphere calculated with a chemistry general circulation model. *J. Geophys. Res.,* **100,** 20 983–20 998.

Rood, R. B., 1987: Numerical advection algorithms and their role in atmospheric transport and chemistry models. *Rev. Geophys.,* **25,** 71–100.

Stockwell, D. Z., and M. P. Chipperfield, 1999: A tropospheric chemical-transport model: Development and validation of the model transport schemes. *Quart. J. Roy. Meteor. Soc.,* **125,** 1747–1783.

Tiedtke, M., 1989: A comprehensive mass flux scheme for cumulus parameterization in large-scale models. *Mon. Wea. Rev.,* **117,** 1779–1800.

von Kuhlmann, R., M. G. Lawrence, P. J. Crutzen, and P. J. Rasch, 2003a: A model for studies of tropospheric ozone and nonmethane hydrocarbons: Model description and ozone results. *J. Geophys. Res.,* **108,** 4294, doi:10.1029/2002JD002893.

——, ——, ——, and ——, 2003b: A model for studies of tropospheric ozone and non-methane hydrocarbons: Model evaluation of ozone related species. *J. Geophys. Res.,* **108,** 4729, doi:10.1029/2002JD003348.

Xie, S., and Coauthors, 2002: Intercomparison and evaluation of cumulus parameterizations under summertime midlatitude continental conditions. *Quart. J. Roy. Meteor. Soc.,* **128,** 1095–1135.

Yanai, M., S. Esbensen, and J. Chu, 1973: Determination of bulk properties of tropical cloud clusters from large-scale heat and moisture budgets. *J. Atmos. Sci.,* **30,** 611–627.

Yano, J.-I., F. Guichard, J.-P. Lafore, J.-L. Redelsperger, and P. Bechtold, 2004: Estimations of mass fluxes for cumulus parameterizations from high-resolution spatial data. *J. Atmos. Sci.,* **61,** 829–842.

Zhang, G. J., 2002: Convective quasi-equilibrium in midlatitude continental environment and its effect on convective parameterization. *J. Geophys. Res.,* **107,** 4220, doi:10.1029/2001JD001005.

——, 2003: Convective quasi-equilibrium in the tropical western Pacific: Comparison with midlatitude continental environment. *J. Geophys. Res.,* **108,** 4592, doi:10.1029/2003JD003520.

——, and N. A. McFarlane, 1995: Sensitivity of climate simulations to the parameterization of cumulus convection in the Canadian Climate Centre general circulation model. *Atmos.–Ocean,* **33,** 407–446.